

Spray pyrolysis deposited zinc oxide films for photo-electrocatalytic degradation of methyl orange: influence of the pH

M. Quintana^a, E. Ricra^a, J. Rodríguez^{b,*}, W. Estrada^b

^a Facultad de Ciencias, Universidad Nacional de Ingeniería, P.O. Box 31-139, Av. Tupac Amaru 210, Lima, Peru

^b Instituto Peruano de Energía Nuclear, Av. Canada 1470, Lima, Peru

Abstract

Zinc oxide films were made by spray pyrolysis equipped with an optical system for in situ thickness measurement. Films were fabricated from zinc acetate water solution. The solution's pH was modified to increase film porosity, which was subsequently analyzed using scanning electron microscopy. X-ray diffractometry revealed that resulting films were zincite-like with a preferred (002) direction depending on the temperature of deposition. Spectral optical equipment analyzed the absorption of ZnO based films in the 350–800 nm. The various zinc oxide films were brought in contact with methyl orange, whose photo-electrocatalytically induced degradation under ultraviolet irradiation was investigated in a reactor allowing optical probing of methyl orange. Results can be reconciled with the active area's suitability for producing photoinduced holes capable of effecting oxidation of the pollutant.

© 2002 Elsevier Science B.V. All rights reserved.

Keywords: Methyl orange; Photo-electrocatalytic degradation; Zinc oxide films

1. Introduction

Heterogeneous photocatalysis is a topic of major and growing importance [1]. It can be used for the decomposition of hazardous wastes, which in the case of textiles, pose a serious problem in Third World Countries. Titanium oxide is the primary study material for these applications [1–3]. However, zinc oxide can in principle be used as well [4–6], its energy bands being appropriate for water purification [7]. In the case of thin films, high porosity is strongly recommended as they are capable of a very large interface with fluids. Preparation of zinc oxide films has been the subject of continuous research. Different techniques have been

reported for preparing this material; including reactive evaporation [8], sputtering [9], chemical bath [10], spray pyrolysis [11–14], etc. Spray pyrolysis deposits most of the intrinsic zinc oxide films by pyrolytic decomposition of alcoholic solution of zinc acetate. Alcoholic solutions were preferred because their low surface tension and viscosity facilitate the formation of small spray droplets while their low boiling point enables them to be efficiently removed. It is expected that using water as solvent will increase film porosity. Photocatalysis involves excitation of an electron from the valence band to the conduction band; the remnant hole migrates under the influence of the electric field towards the surface of the semiconductor and reaches a site where it can oxidize an electron donor associated with the pollutant. Reportedly, a decrement of the electron-hole recombination can be obtained by an

* Corresponding author. Fax: +511-4810824.

E-mail address: jrodriguez@uni.edu.pe (J. Rodríguez).

applied potential, which increases the migratory effects in the semiconductor–electrolyte interface [15–17].

This paper discusses thin film manufacturing including film characterization with respect to morphology and structure. Optical measurements and photo-electrochemical characterization of the photo-catalytic zinc oxide films in contact with a solution containing methyl orange were performed. Specifically, we study in situ absorbance spectra taken at different degradation times and find enhanced degradation rates of methyl orange in films. These results are correlated with an increment of film porosity depending on deposition conditions.

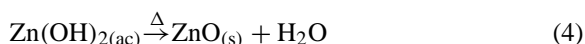
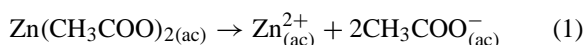
2. Experimental

Zinc oxide films were deposited using reactive spray pyrolysis in a home made system (Fig. 1). The depositing solution is placed in an ultrasonic device which is activated by an air pump equipped with a manometer to measure the applied pressure. In all the experiments

the deposition pressure of the films was 25 psi. Passing through the nozzle, the cloud formed will reach the hot substrate. In the hot substrate, solvent evaporation occurs and the film starts to grow.

In order to ensure a homogeneous film, the substrate placed on the heater is moved back and forth perpendicularly to the deposition nozzle. A mounted in situ optical thickness analyzer is activated by a 632.8 nm wavelength laser beam. The system includes multiple sensors which provide information of the transversal variation in film thickness.

Films deposition takes place according to the following reactions:



The films were deposited onto a Libbey Owens Ford glass precoated with a layer of transparent $\text{SnO}_2\text{:F}$

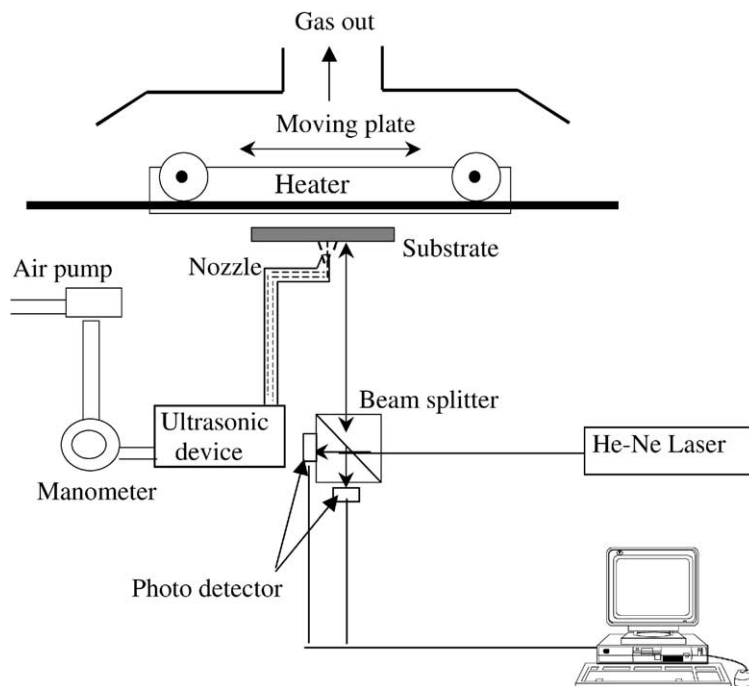


Fig. 1. Spray pyrolysis deposition system including the optical set-up for coating profile measurement.

with square of $8\ \Omega$ resistance. During deposition, the substrates were kept at temperatures in the range from 300 to 400 °C, and at varying pH. The optical system presented in Fig. 1 determined a film thickness of ~ 650 nm in situ during the deposition.

3. Results and discussion

3.1. Film characterization: structure and morphology

The crystalline structure of the zinc oxide films was studied by X-ray diffraction (XRD) using a Phillips Xpert 1300 diffractometer with Cu anode. Data from ZnO standards were used to identify the diffraction peaks. Fig. 2 shows X-ray diffractograms for zinc oxide films deposited at different temperatures and various pHs onto SnO₂:F coated glass substrates.

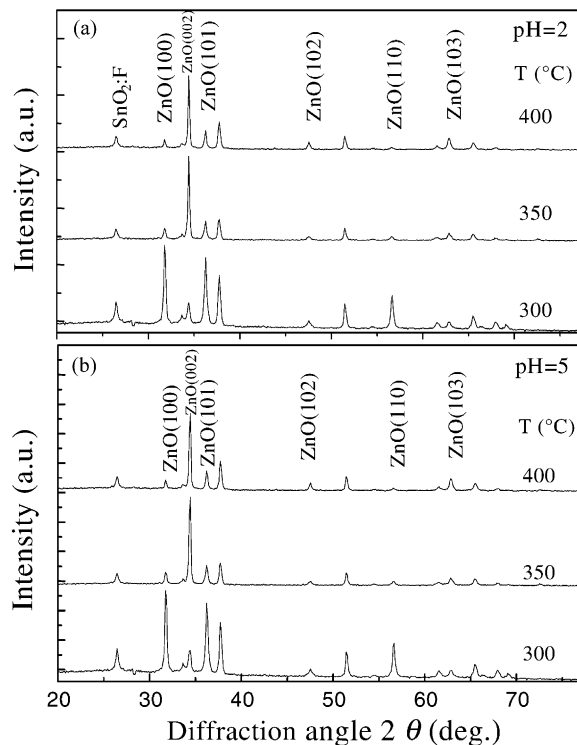


Fig. 2. X-ray diffractograms for zinc oxide films prepared by spray pyrolysis at pH 2 (panel a) and pH 5 (panel b), and at the shown temperatures. The observed peaks correspond to the zincite structures. Additional peaks are due to the transparent conductive layer of SnO₂:F.

The diffractograms display that, regardless of the pH values, the crystalline structure in zincite-like films appears in the range temperature between 300 and 400 °C. For films prepared at 300 °C, parallel planes in the (1 0 0), (1 0 1) and (1 1 0) directions can be observed. As the deposition temperature increases, the (0 0 2) direction is preferred vis-a-vis other directions, which start then to decrease.

The mean grain size D for the films was estimated from the XRD data by applying Scherrer's formula as follows:

$$D = \frac{0.9\lambda_x}{\beta \cos \theta} \quad (5)$$

where λ_x is the X-ray wavelength in the K α band for Cu equal to 1.54 Å, and β is the full width at half the maximum diffraction peak. Applying this formula, the grain size was found to be ~ 23 nm measured in the (0 0 2) peak.

Surface morphology was studied with SEM using a Philips 300 instrument operated at 20 kV. Figs. 3 and 4 display the surface of zinc oxide films deposited at different temperatures and pHs onto a conductive transparent layer of SnO₂:F, respectively. Fig. 3 is observed that increasing deposition temperature, increase the particles size until transform it in round nodules reducing in that sense the surface area. Fig. 4 is observed that pH variation on the deposition conditions of zinc oxide films produce a change of shape in the particles, from planar, obtained in films deposited at pH 2, to round, obtained in films deposited at pH 5. An increase of film's surface area is observed at the last case.

3.2. Film characterization: optical properties

For zinc oxide films deposited onto glass at 400 °C and different pH values, total normal transmittance was recorded in the $350 < \lambda < 800$ nm wavelength range with an Optometrics RS-350 single beam spectrophotometer. Films were ~ 650 nm thick, as observed with the in situ thickness measurement system mounted in the deposition system.

As a general trend, it is observed that decrements of transmittance appear as the pH in the solution increases. They are correlated with the increment of the films' diffusive characteristics, which can be due to the fact that spherical particles obtained at pH 5 are

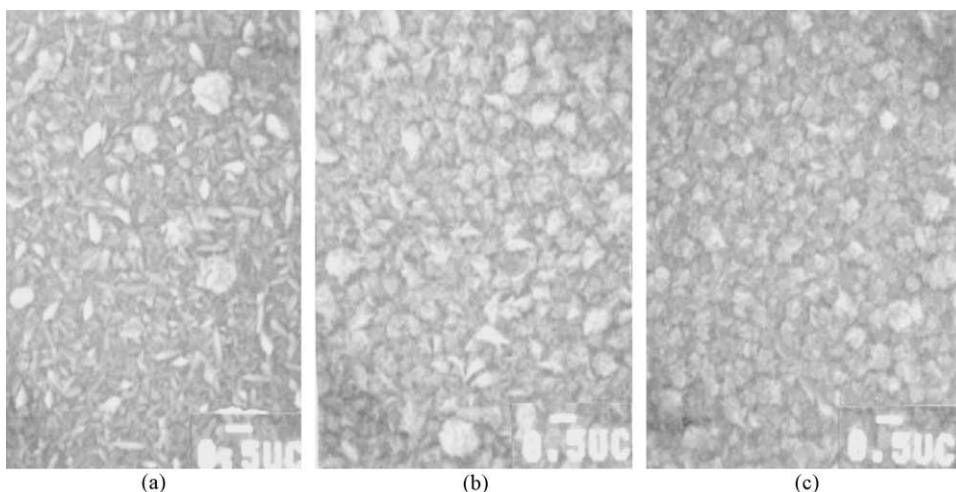


Fig. 3. SEM image of the surface of zinc oxide films deposited by spray pyrolysis at 400°C onto a conductive transparent layer of SnO:F coated glass. Film deposited at pH 5, with the following temperatures: (a) $T = 300^\circ\text{C}$; (b) $T = 350^\circ\text{C}$; and (c) $T = 400^\circ\text{C}$.

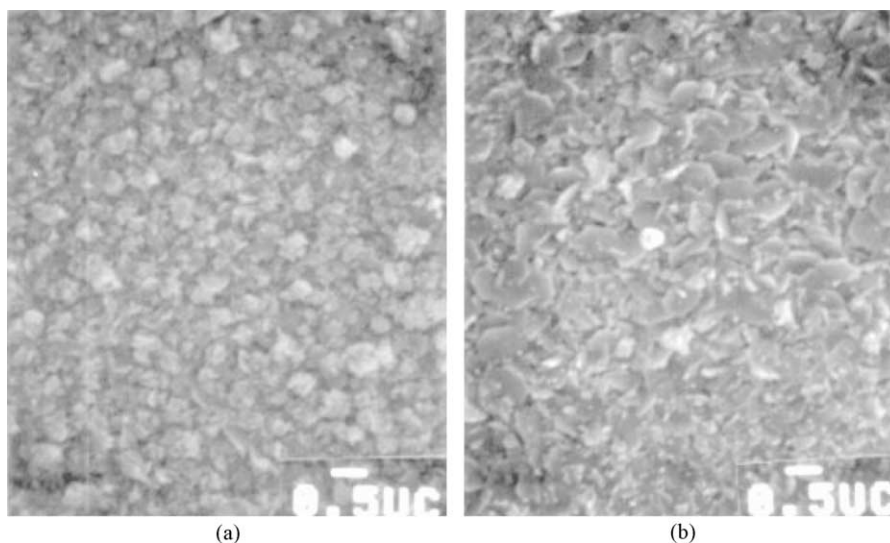


Fig. 4. SEM image of the surface of zinc oxide films deposited by spray pyrolysis at 400°C onto a conductive transparent layer of SnO:F coated glass. Films deposited at pH 5 (panel a) and pH 2 (panel b).

more light dispersive than planar particles obtained at pH 2, as shown in Fig. 5.

3.3. Data on photo-electrocatalytic degradation of methyl orange

We used zinc oxide films to study the photo-electrocatalytic degradation of a methyl orange water solu-

tion by using a specially designed reactor. The reactor consists of a cylindrical Teflon container. The open end—which can be irradiated by ultraviolet (UV) light—has provisions for mounting a sample with the zinc oxide film facing the interior of the cylinder. Light passing through the conductive transparent substrate will make then possible to illuminate the zinc oxide films. Two parallel quartz windows are arranged

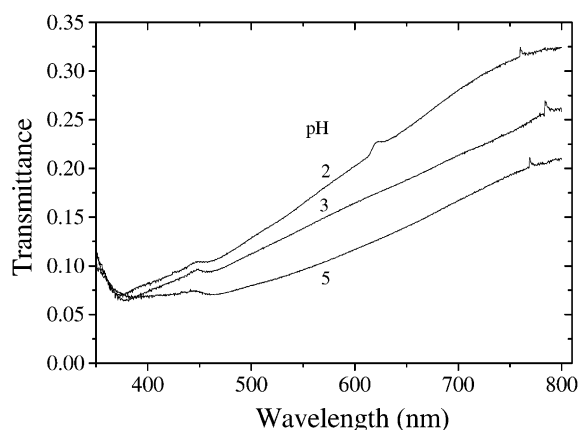


Fig. 5. Spectral measured transmittance for zinc oxide films deposited on glass by spray pyrolysis at 400 °C and at the shown pHs.

at right angles to the cylinder axis so as to allow spectrophotometric transmittance measurements for probing the cylinder's contents. A three-electrode arrangement was used in the experiments. It includes a Pt foil as counter electrode, and a Ag/AgCl electrode as a reference electrode. This setup is referred to as a "single compartment cell" in earlier work by us [17].

The experimental data, to be reported below, were obtained with 8 ml KCl 0.1 M in the container, in the case of photocurrent measurements (Figs. 6 and 7), and of 35×10^{-5} M methyl orange in the container, in the case of photocatalytic degradation of methyl orange. In the latter case, a distilled water solution with pH 5.5 was used. Irradiation was accomplished with a Phillips Hg 250 W lamp mounted 15 cm in front of the sample. In order to avoid thermal effects, a water filter was mounted between the lamp and the photoreactor. The intensity in the UV-A spectrum (315–400 nm)—measured with an UDT 300 radiometer—was 3 mW. The photoreactor was positioned in the sample compartment of a RS-325 Optometrics Single beam spectrophotometer operating at $350 < \lambda < 800$ nm. A mechanical chopper system was employed to avoid UV irradiation during the spectrophotometer recordings. Electrochemical measurements were taken with a Wenking POS 73 potentiostat interfaced to a computer. Experiments were performed at 10 mV/s. In the dark non electrochemical reactions were observed in the -1 to 1 V scanned range.

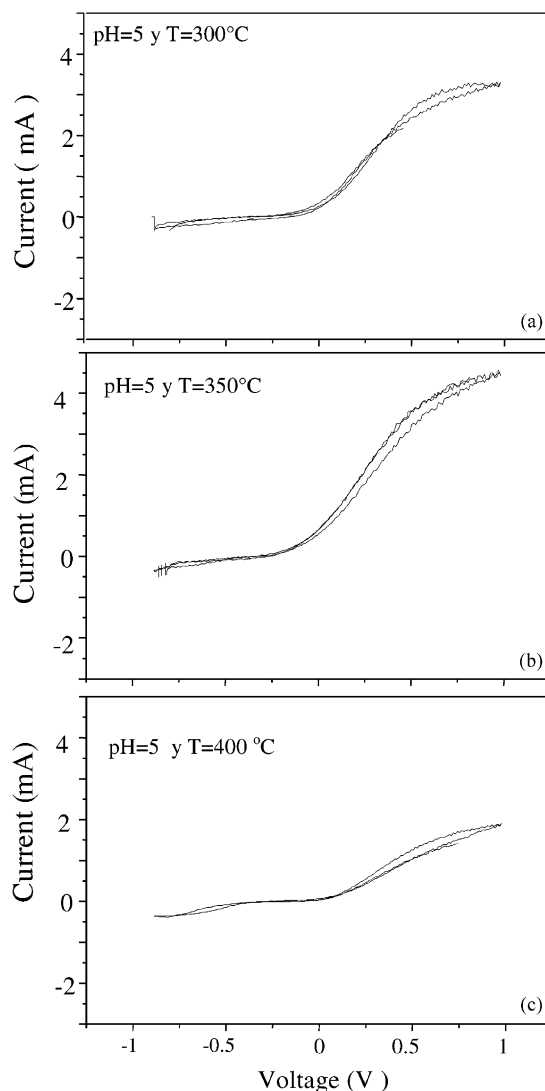


Fig. 6. Cyclic voltammograms obtained under UV irradiation for zinc oxide films prepared at pH 5 and at the shown temperatures: (a) $T = 300$ °C; (b) $T = 350$ °C; and (c) $T = 400$ °C. Experiments were performed at 10 mV/s. Plots show the fifth cycle in each experiment.

In Figs. 6 and 7, cyclic voltammograms show the effect of the deposition parameters: temperature and pH on the photoactivity of zinc oxide films.

Experiments were performed under UV illumination. In the dark, the obtained current across the scanned range was zero before and after illumination. Fig. 6 shows films deposited at 400 °C present

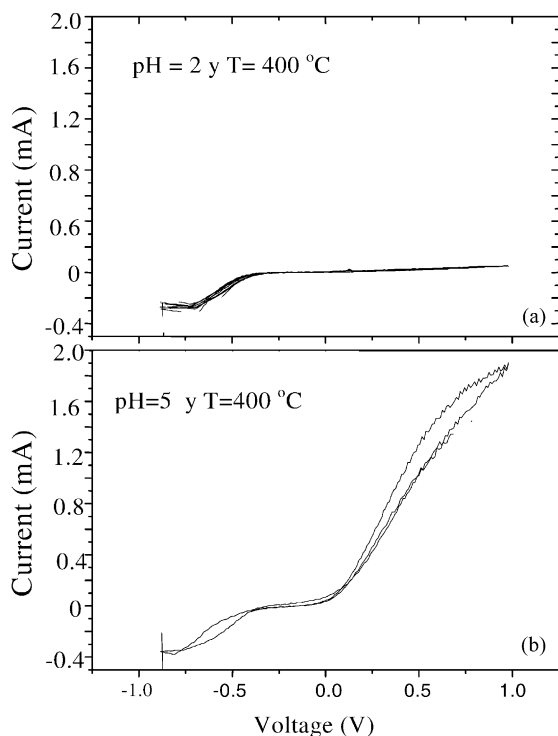


Fig. 7. Cyclic voltammograms obtained for zinc oxide films under UV irradiation. Films were prepared at 400 °C, with the shown pH values: (a) pH 2; (b) pH 5. Experiments were performed at 10 mV/s. Plots show the fifth cycle in each experiment.

slightly lower photocurrent that films deposited at lower temperatures. In Fig. 7, a dramatic increment in the photocurrent is observed when the pH of the deposition conditions is increased.

An applied bias potential of 0.7 V versus the Ag/AgCl reference electrode was used to avoid electron-hole recombination in the irradiated samples; this effect may otherwise be significant, mainly as a consequence of traps and surface states. In order to diminish the influence of free oxygen, a well-known electron scavenger, nitrogen bubbles were introduced continuously into the sample compartment, so that the solution was kept uniformly mixed. Fig. 8 shows the resulting photocurrent in a typical experiment of methyl orange 35×10^{-5} M obtained using two zinc oxide films as photocatalyst. It may be seen that for the films deposited pH 5, the photocurrent is higher than for those deposited at pH 2. However, a consistent decrement as a function of time is observed in the

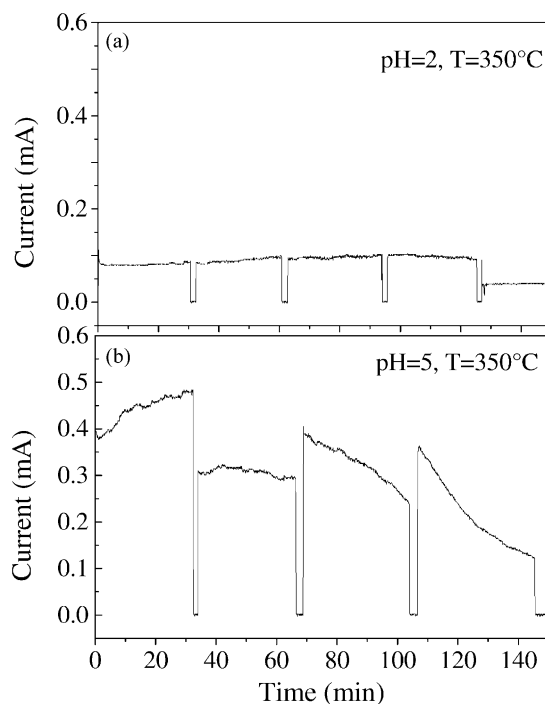


Fig. 8. Photocurrent as a function of time for UV irradiated 650 nm thick zinc oxide films in a 35×10^{-5} M of methyl orange water solution. The data pertain to the shown pH deposited values of the zinc oxide films: (a) pH 2; (b) pH 5.

films deposited at pH 5, probably due to limitations in the diffusion of dye from the bulk of the solution into the semiconductor.

Reaction products such as hydrazine are expected to appear as a result of the photocatalytic degradation of methyl orange [18]. These products, as well as the methyl orange itself, display characteristic optical absorption at 460 and ~ 245 nm, respectively. The latter substance is an intermediate of the photo-electrocatalytic degradation of methyl orange to harmless products so they can be identified by spectrophotometry. Fig. 9a and b shows typical absorbance spectra of the methyl orange solution during photo-electrocatalysis with zinc oxide films prepared at different pHs under UV irradiation. A 0.7 V of anodic potential was applied. Photocurrent measured values were presented in Fig. 8.

The spectral data display pronounced absorption at ~ 460 nm due to methyl orange. Fig. 9a shows, for the case of films prepared at pH 2, that this absorption

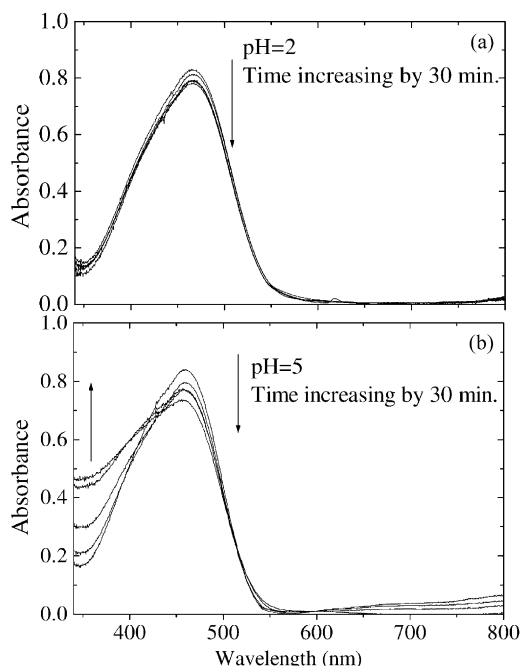


Fig. 9. Spectral absorbance measured after UV irradiation for the shown times in order to degrade 35×10^{-5} M of methyl orange. The data pertain to the shown pH deposited values of zinc oxide films: (a) pH 2; (b) pH 5.

drops slightly under UV irradiation. However, for pH 5 presented in Fig. 9b, the absorption drops monotonically, concomitantly with an increase of the absorption at 350 nm, probably due to an hydrazine derivative. However, more research is needed in this case. Intermediates of the photo-electrocatalytic degradation, have been observed to increase in concentration at the beginning of the photocatalytic reaction. They, as in the case of hydrazine can disappear after hours in air solutions [18] or can be photodegraded during the photo-electrocatalysis in a parallel process.

Fig. 10 shows the relative concentration of the methyl orange during its photo-electrocatalytic degradation using zinc oxide irradiates with UV. The data are based on the intensity of the absorption at $\lambda = 460$ nm of experiments shown in Figs. 8 and 9.

It is evident that thin film manufacturing plays an important role in photodegradation. After ~ 3 h, the concentration of methyl orange in the solution has decreased only a quarter of the initial concentration in the best of the cases. We note that the

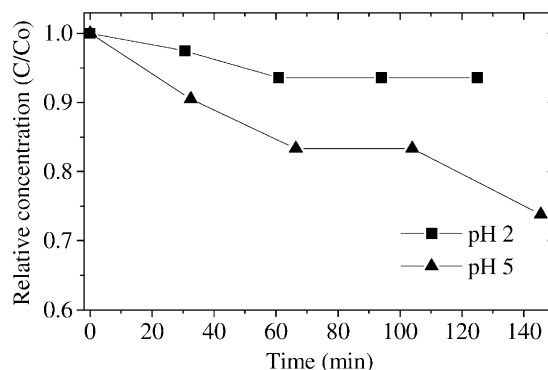


Fig. 10. Relative concentration calculated after UV irradiation for the shown times in order to degrade 35×10^{-5} M of methyl orange. The data was obtained at $\lambda = 460$ nm and pertain to the shown pH deposited values of zinc oxide films: (a) (■) pH 2; (b) (▲) pH 5.

photo-electrocatalytic degradation rate correlates with the optical absorption at short wavelengths, as evident from Fig. 5. We should point out that for the used lamp, the maximum of the irradiation spectra is around 350 nm, matching a minimum of the methyl orange absorption. This can explain why UV light without zinc oxide cannot degrade the methyl orange. In addition, illuminating the films through the substrate will cut off the irradiation below 300 nm, due mainly to the glass absorption, shadowing most of the absorption of the zinc oxide films.

4. Conclusions

We prepared zinc oxide films by spray pyrolysis under conditions giving high porosity films. Films deposited at low pH values have shown to be more compact and do not present much photoactivity, compared with films deposited at higher values. In the range of the used deposition temperatures, from 300 to 400 °C, a preferred structural (002) direction is observed. A slight decrement in photoactivity can be seen in films deposited at 400 °C compared to those deposited at 350 °C, due to crystal growth and a smaller surface area.

The photo-electrocatalytic ability of the films to degrade methyl orange was investigated in detail in a reactor allowing optical measurements to document the presence of methyl orange as well as the

intermediated reaction product hydrazine. Degradation rates have shown to be more efficient with films deposited at high pH values, thus favoring the increment of the film's surface area.

Acknowledgements

We want to thank the International Science Programme at Uppsala University (Sweden), the Facultad de Ciencias, Universidad Nacional de Ingenieria and IPEN for providing partial funding for this project. C. Luyo is thanked for the SEM pictures.

References

- [1] D.M. Blake, Bibliography of work on the heterogeneous photocatalytic removal of hazardous compounds from water and air, NREL/TP-510-31319, 2001.
- [2] A. Fujishima, K. Hasimoto, T. Watanabe, in: A. Donald, Y. Kitamura, N. Tamaki (Eds.), *TiO₂ Photocatalysis, Fundamentals and Applications*, BKC, Tokyo, Japan, 1999.
- [3] M. Hoffmann, S. Martin, W. Choi, D. Bahnemann, *Chem. Rev.* 95 (1995) 69.
- [4] X. Domenech, J. Peral, *Chemosphere* 38 (6) (1999) 1265.
- [5] B. Neppolian, S. Sakthivel, B. Arabindo, M. Palanichamy, V. Murugesan, *J. Environ. Sci. Health A: Toxic/Hazard. Subst. Environ. Eng.* A34 (1999) 1829.
- [6] G. Marci, V. Augugliaro, M.J. Lopez-Muñoz, C. Martin, L. Palmisano, V. Rives, M. Schiavello, R. Tilley, A. Venezia, *J. Phys. Chem. B* 105 (2001) 1026.
- [7] N. Serpone, P. Maruthamuthu, P. Pichat, E. Pelizzetti, H. Hidaka, *J. Photochem. Photobiol. A* 85 (1995) 247.
- [8] S. Nasseem, M. Iqbal, K. Hussain, *Sol. Energy Mater.* 31 (1993) 155.
- [9] A. Krzesinsky, *Thin Solid Films* 138 (1986) 111.
- [10] M. Ristov, G.J. Sidaninovskiy, Y. Grozdanov, M. Mitreski, *Thin Solid Films* 148 (1987) 65.
- [11] C.H. Lee, L.Y. Lin, *Appl. Surf. Sci.* 92 (1996) 163.
- [12] M. Krunk, E. Melikov, *Thin Solid films* 270 (1995).
- [13] H. Gomez, A.A. Maldonado, R. Asomoza, E.P. Zironi, J. Canetas-Ortega, J. Palacios-Gomez, *Thin Solid Films* 293 (1997) 117.
- [14] A.S. Riad, S.A. Mahmoud, A.A. Ibrahim, *Physica B* 296 (2001) 319.
- [15] K. Vinodgopal, S. Hotchandani, P.V. Kamat, *J. Phys. Chem.* 97 (1993) 9040.
- [16] K. Vinodgopal, U. Stafford, K.A. Gray, P.V. Kamat, *J. Phys. Chem.* 98 (1994) 6797.
- [17] J. Rodriguez, M. Gomez, S.E. Lindquist, C.G. Granqvist, *Thin Solid Films* 360 (2000) 250.
- [18] T.B. Graham, J.R. Darwent, *J. Chem Soc., Faraday Trans. 1* (83) (1989) 1631.